Electronic analogy of Goos-Hänchen effect: a review

Xi Chen[1,2], Xiao-Jing Lu[1], Yue Ban[2], and Chun-Fang Li[1]

[1] Department of Physics, Shanghai University, 200444 Shanghai, China

[2] Departamento de Química-Física, UPV-EHU, Apdo 644, 48080 Bilbao, Spain

E-mail: `xchen@shu.edu.cn`

Abstract. The analogies between optical and electronic Goos-Hänchen effects are established based on electron wave optics in semiconductor or graphene-based nanostructures. In this paper, we give a brief overview of the progress achieved so far in the field of electronic Goos-Hänchen shifts, and show the relevant optical analogies. In particular, we present several theoretical results on the giant positive and negative Goos-Hänchen shifts in various semiconductor or graphen-based nanostructures, their controllability, and potential applications in electronic devices, e.g. spin (or valley) beam splitters.

Submitted to: *J. Opt. A: Pure Appl. Opt.*

1. Introduction

The Goos-Hänchen (GH) effect, named after Hermann Fritz Gustav Goos and Hilda Hänchen [1], is an optical phenomenon in which a light beam undergoes a lateral shift from the position predicted by geometrical optics, when totally reflected from a single interface of two media having different refraction indices [2]. The lateral GH shift, conjectured by Isaac Newton in the 18th century [3], was theoretically explained by Artmann's stationary phase method [4] and Renard's energy flux method [5]. With the development of laser beam and integrated optics [2], the GH shift becomes very significant nowadays, e.g. in the applications of optical waveguide switch [6] and sensors [7, 8], or in fundamental problems on tunneling time [9, 10, 11]. Therefore, the GH shift as well as other three nonspecular effects such as angular deflection, focal shift, and waist-width modification have been investigated in various configurations like frustrated total internal reflection (FTIR) [12, 13, 14, 15], attenuated total reflection (ATR) [16, 17], and partial reflection [18, 19, 20, 21, 22, 23], and also extended to other physics fields [2] including nonlinear optics, plasmas, semiconductor, acoustics [24], neutron physics [25, 26] and even atom optics [27].

The considerable number of publications on the subject, and a recent workshop on "Beam Shifts: Analogies between light and matter waves" held at Lorentz Center, Leiden, Netherlands (28 March-1 April 2011) demonstrate much current interest, not only from optics community but also from other fields such as condensed matter and particle physics. In recent years, the lateral GH shift and transverse Imbert-Fedorov (IF) shift (also known as spin-Hall effect of light) [28, 29, 30, 31, 32, 33], have attracted much attention (see review [34]). The field covered here is vast, and we pay special attention to work done by the authors, while making effort to offer a global perspective. Therefore, in this review we shall concentrate on the electronic GH shifts in semiconductor and graphene-based nanostructures and their applications in spin (or valley) beam splitters and filters.

Historically, the study of electronic GH shift is traced back to 1960s [5, 35]. In 1964, Renard [5] proposed the energy flux method to investigate the GH shift for matter waves, based on the analogy between Schrödinger equation in quantum mechanics and Helmholtz equation in electromagnetic theory. Later on, Carter and Hora [35] considered the GH shift of matter waves in total reflection at grazing incidence. Motivated by the progress on optical GH and IF shifts, Miller *et. al.* [36] made a theoretical investigation of the analogous GH shifts of a Dirac electron beam which undergoes a series of total internal reflections from finite potential barriers of arbitrary smoothness. In general, it is found that the GH shift for Dirac electrons is at most of the order of a Compton wavelength. To observe it macroscopically, the GH shift for Dirac electrons was further proposed to be amplified by multiple reflections [37]. However, it is still an open challenge to detect the electric GH shift, due to the smallness of GH shift, and the difficulty in preparation of well-collimated electron beam, the analogue of an optical beam in electronics.

With the advent of techniques for the semiconductor growth and fabrication of semiconductor nanoelectronic devices, the optics-like phenomenon [38], such as reflection, focusing, diffraction, and interference, resulting from the fact that the quantum-mechanical

wave nature of electrons, become prominent in electron wave devices, thus have given rise to a field of research which is best described as ballistic electron optics in two-dimensional electron systems (2DESs) [39, 40]. In 1993, Wilson *et. al.* [41] have studied the GH shift and associated time delay for an electron beam totally reflected from a potential-energy/effective-mass interface in semiconductor. It was found that the phase shift resulting in the GH shift and time delay upon the total internal reflection has great effect on the quantum interference in electron wave devices, and thus contributes to novel electron waveguiding characteristics. Again, the smallness of electronic GH shifts in total reflection has impeded its direct measurement and applications in electron devices. To overcome this bottleneck, we generalized the electronic GH shift in total internal reflection to that in partial reflection [42, 43]. The resonance-enhanced GH shift of ballistic electrons in transmission was found in semiconductor quantum barrier [42] as well as quantum well [43]. More interestingly, the lateral shifts of electron beam transmitted through a semiconductor quantum well, acting as electron wave slab, can be negative and positive, depending on the incidence angle [43]. Moreover, the negative and positive GH shifts separate the spin-up electron beam from spin-down electron beam spatially in a more realistic setup, i. e., parabolic potential well under a uniform vertical magnetic field [44] and δ-magnetic barrier nanostructures [45]. This achievement leads to some other interesting investigations and applications in quantum electronic devices such as spin filter or spin beam splitter. For instance, the GH shift in magnetic-electic nanostructures can be utilized to design a spin beam splitter, when the GH shift can be controlled by adjusting the electric potential induced by applied voltage and magnetic field strength of ferromagnetic stripes [45]. For recent developments on this line of research, we refer the readers to the references [46, 47, 48, 49].

A different but relevant line is electronic GH shift in graphene [50, 51, 52, 53, 54, 55, 56, 57, 58]. The first experimental fabrication of monolayer graphene [59, 60], the graphitic sheet of one-atom thickness, has inspired many interesting and new concepts on Dirac electron optics to design graphene-based electron wave devices [61]. Motivated by electronic negative refraction, Veselago lens and foucusing in graphene [62], Beenakker and his collaborators [50] have pioneered the quantum GH effect at *p-n* interface in graphene, and have shown that the electronic GH shifts result in a remarkable $8e^2/\hbar$ conductance plateau in *p-n-p* graphene junction. This work stimulates other progress on resonance-enhanced GH shifts in various graphen-based nanostructures, including single [52], (asymmetric) double barrier [53], and superlattice [54]. These huge (negative or positive) GH shifts are considered to be more suitable to design the controllable valley and spin beam splitter. Similar to those in semiconductor, the GH shifts in graphene can be also modulated by electric and magnetic barriers [55], which influences the electronic transport in graphene-based electronics. Besides, a different and intriguing phenomenon is that the GH shifts can be also controlled by using only strain, without requiring any external fields [56, 57]. In strained graphene, the lateral shifts, depending on stain tensor and direction [58], lead to valley-dependent transports and graphene-based valleytronic devices like valley beam splitter [57].

The review is organized as follows. In Sec. 2 and 3, we shall present the work on GH shifts in semiconductor and graphene nanostructures, respectively. Throughout this review,
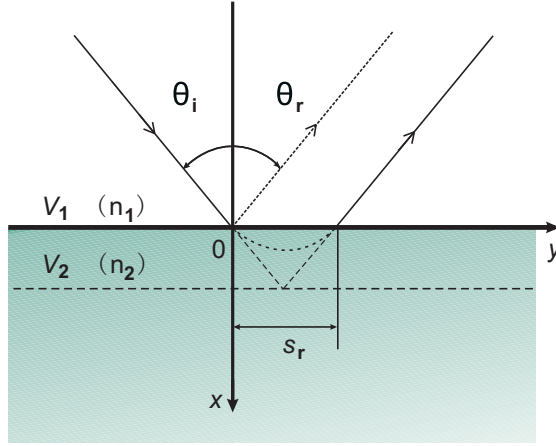
Figure 1. (Color online) Schematic diagram of an electron beam totally reflected from a single potential energy/effective mass interface with a lateral GH shift, s_r. The incident, reflected are schematically represented by their respective beam axis. The dotted line is the path expected from the geometrical result in electron optics.

we attempt to establish analogies between GH shifts of light beams and electron beams in semiconductor or graphene, and address such issues as (i) the properties of GH shifts in reflection and transmission, (ii) their controllability, and (iii) their dependence on different degrees of freedom, e. g. spin or valley. Some remarks and prospects will be presented in Sec. 4.

2. Electronic Goos-Hänchen shifts in semiconductor

2.1. single interface

We shall start with the GH shift for the totally reflected electron beam at a single interface between two different potential energies in semiconductor, which helps to establish the analogy of optical and electronic GH shifts on a heuristic basis. As shown in Fig. 1, we consider a ballistic electron beam of total energy E that is incident at an incidence angle θ_0 from one region to the other, where the conduction band edge potential energies are V_1 and V_2 ($V_1 < V_2$), and the effective mass are m_1^* and m_2^*, respectively. When the incidence angle θ_0 is lager than the critical angle

$$\theta_c = \sin^{-1} \sqrt{\frac{m_2^*(E - V_2)}{m_1^*(E - V_1)}}, \tag{1}$$

the total internal reflection will happen. The critical angle for total reflection are valid for the potential step (rise), when the energy satisfies $V_2 < E < E_c$ with $E_c = (m_2^*V_2 - m_1^*V_1)/(m_2^* - m_1^*)$ [41]. In this case, the reflectivity and phase shift are respectively given by

$$r = \frac{1 - i\frac{m_1^*\kappa}{m_2^*k_x}}{1 + i\frac{m_1^*\kappa}{m_2^*k_x}} = e^{i\phi_r}, \tag{2}$$

and

$$\phi_r = -2 \tan\left(\frac{m_1^* \kappa}{m_2^* k_x}\right), \tag{3}$$

where $k_x = k\cos\theta$, $k_y = k\sin\theta$, $\kappa = (k_y^2 - k'^2)^{1/2}$, $k = [2m_1^*(E - V_1)]^{1/2}/\hbar$ and $k' = [2m_2^*(E - V_2)]^{1/2}/\hbar$. Here θ is the incidence angle for the plane-wave component under consideration. Now we are ready to calculate the GH shift for a finite-sized electron beam. The wave function of the incident beam is assumed to be

$$\Psi_{in} = \frac{1}{\sqrt{2\pi}} \int_{-\infty}^{\infty} A(k_y - k_{y0}) \exp[i(k_x x + k_y y)] dk_y, \tag{4}$$

with the angular spectrum distribution $A(k_y - k_{y0})$ around the central wave vector k_{y0}. The wave function of the reflected one is thus expressed as

$$\Psi_r = \frac{1}{\sqrt{2\pi}} \int_{-\infty}^{\infty} r(k_y) A(k_y - k_{y0}) \exp[i(-k_x x + k_y y)] dk_y, \tag{5}$$

where $r(k_y)$ is given by Eq. (2). In practice, the range of the above integral is from $-k$ to k, and here it can be ideally extended from $-\infty$ to ∞ for a well-collimated electron beam.

To find the position where $|\Psi_r|^2$ is maximum, that is, the GH shift of the reflected beam, we look for the position at which the total phase $\Phi = -k_x x + k_y y + \phi_r$, has an extremum when differentiated with respected to k_y, that is to say, $\partial\Phi/\partial k_y = 0$ [63]. This provides the stationary-phase expression of GH shift, namely,

$$s_r = -\frac{\partial\phi_r}{\partial k_y}\Big|_{\theta=\theta_0}, \tag{6}$$

which yields the electronic GH shift in total reflection [41, 42]

$$s_r = \frac{2}{\kappa_0} \frac{(k^2 - k'^2)\tan\theta_0}{(m_1^*/m_2^*)\kappa_0^2 + (m_2^*/m_1^*)k_{x0}^2}, \tag{7}$$

where the subscript 0 denotes the value taken at $\theta = \theta_0$, namely $k_y = k_{y0}$. This demonstrates that there exists the GH shift for ballistic electrons in semiconductor. So far, spin is totally neglected in our discussions. Since the GH shift is proportional to the de Broglie wavelength, $1/\kappa_0$, it is a purely wave-like effect, and has nothing to do with the spin-orbit coupling. Like the GH shift in optics, the electronic GH shift in total internal reflection is only about the order of the electron wavelength, which has impeded its direct measurement and applications in electron devices. This drawback motivates us to study the enhancement of electronic GH shifts, see below.

The close analogy between ballistic electrons transport (electron wave propagation) in semiconductor and the electromagnetic wave propagation in classical optics has been well established [39, 64]. The similarity and difference for electron wave and electromagnetic wave are shown in Table 1. As shown in Fig. 1, we can calculate the GH shift of light beam totally reflected from a single interface of two media having different refraction indices, $n_1 = \sqrt{\mu_1 \varepsilon_1}$ and $n_2 = \sqrt{\mu_2 \varepsilon_2}$,

$$s_r^{TE} = \frac{2}{\kappa_0} \frac{(k^2 - k'^2)\tan\theta_0}{(\mu_1/\mu_2)\kappa_0^2 + (\mu_2/\mu_1)k_{x0}^2}, \tag{8}$$

$$s_r^{TM} = \frac{2}{\kappa_0} \frac{(k^2 - k'^2)\tan\theta_0}{(\varepsilon_1/\varepsilon_2)\kappa_0^2 + (\varepsilon_2/\varepsilon_1)k_{x0}^2}, \tag{9}$$

Table 1. Analogy for the electron wave and classical optics

Electron wave	TE wave	TM wave
$\nabla^2\Psi = -(2m/\hbar)(E - V)\Psi$	$\nabla^2 E = -\omega^2\mu\varepsilon E$	$\nabla^2 H = -\omega^2\mu\varepsilon H$
$k^2 = 2m(E - V)/\hbar$ (parabolic)	$k^2 = \omega^2\mu\varepsilon$ (linear)	$k^2 = \omega^2\mu\varepsilon$ (linear)
$2(E - V)/\hbar$	ω	ω
m	μ	ε
$1/[2(E - V)]$	ε	μ

which are the same as Eq. (7). With the analog parameters in Table 1, we have $k = \sqrt{\mu_1\varepsilon_1}\omega$ and $k' = \sqrt{\mu_2\varepsilon_2}\omega$ are the wave vector in two different media, and other parameters are expressed as $\kappa = (k_y^2 - k'^2)^{1/2}$, $k_x = k\cos\theta$, and $k_y = k\sin\theta$ in optical analogy, respectively. Apart from the similarity, we should also point out the difference in the electron effective masses brings new degree of freedom, and as a result the critical angle, reflection, transmission, and GH shift are more complicated and also interesting. For instance, when the negative effective electron mass is considered in a semiconductor, e.g. *GaN* [65], the electronic analogy of negatively refractive media can be achieved, and the GH shift of ballistic electrons is expected to be negative [66].

2.2. quantum barrier and well

Based on the previous results [41, 42], the GH shift in total reflection can be further generalized to partial transmission in semiconductor quantum barrier and well, as shown in Fig. 2. First of all, we turn to discuss the GH shift in transmission through a semiconductor quantum barrier, extending from 0 to a, where $V_2 > V_1$, V_2 is the height of potential barrier, V_1 are the potential energies on its two sides, and corresponding electron effective masses are m_2^* and m_1^*. In this case, the critical angle for total reflection is given by Eq. (1), so that the electron wave propagation inside the region of barrier can be divided into two cases: evanescent and propagating waves. Different from the GH shift in total reflection, the GH shift in transmission though potential barrier can be enhanced by transmission resonances [42], where the potential barrier is described in Fig. 2 (b). Therefore, we just emphasize the propagating case when the incidence angle θ_0 is less than the critical angle θ_c [see Eq. (1)] for total reflection. In this case, the GH shift of the transmitted beam is easily obtained by stationary phase method

$$s = -\frac{\partial\phi}{dk_y}\Big|_{\theta=\theta_0}, \tag{10}$$

where the phase ϕ is given

$$\tan\phi = \frac{1}{2}\left(\frac{m_2^* k_x}{m_1^* k_x'} + \frac{m_1^* k_x'}{m_2^* k_x}\right)\tan k_x' a, \tag{11}$$

where $k_x' = k'\cos\theta'$, $k' = [2m_2^*(E - V_2)]^{1/2}/\hbar$, and θ' is determined by Snell's law for electron wave, $\sin\theta'/\sin\theta = [m_1^*(E - V_1)/m_2^*(E - V_2)]^{1/2}$. Thus, the GH shift in transmission has the
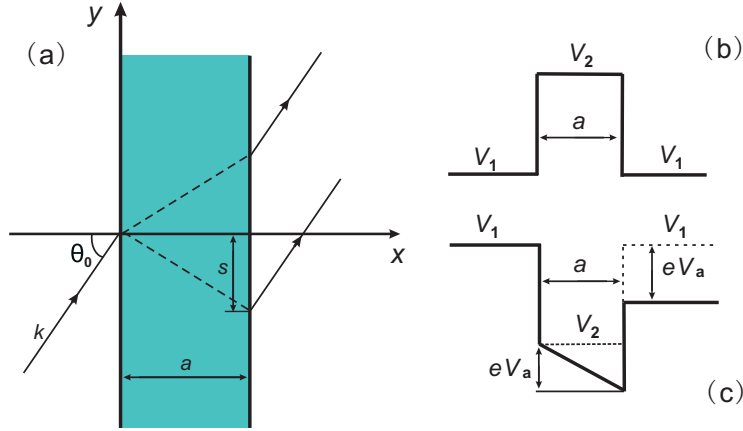
Figure 2. (Color online) (a) Schematic diagram of (positive and negative) lateral GH shifts of ballistic electrons propagating obliquely through a quantum barrier or well, corresponding to a two-dimensional semiconductor potential barrier (b) and well under external applied electric field (c).

following form:

$$s = \frac{s_g}{2f_0^2}\left[\left(\frac{m_2^* k_{x0}}{m_1^* k_{x0}'} + \frac{m_1^* k_{x0}'}{m_2^* k_{x0}}\right) - \left(1 - \frac{k_{x0}'^2}{k_{x0}^2}\right)\left(\frac{m_2^* k_{x0}}{m_1^* k_{x0}'} - \frac{m_1^* k_{x0}'}{m_2^* k_{x0}}\right)\frac{\sin 2k_{x0}'^2 a}{2k_{x0}'^2 a}\right],\tag{12}$$

where $s_g = a\tan\theta_0'$ is the shift predicted from Snell's law for electron waves, and $T_0 = 1/f_0^2$ is the transmission probability, determined by the following complex number,

$$f e^{i\phi} = \cos k_x' a + \frac{i}{2}\left(\frac{m_2^*}{m_1^*}\frac{k_x}{k_x'} + \frac{m_1^*}{m_2^*}\frac{k_x'}{k_x}\right)\sin k_x' a.$$

In the evanescent case where the incident angle θ_0 is larger than the critical angle θ_c, the above expression is still valid, only if k_{x0}' is replaced by $i\kappa_0$. Importantly, the GH shift in this case becomes independent of barrier's thickness, and saturates a constant, which is the order of electron wavelength. This phenomenon is similar to the optical GH shift and associated with Hartman effect in FTIR [14, 15], Here we are more interested in the GH shift in the propagating case, instead of evanescent case.

When $k_{x0}'a = m\pi$ ($m = 1, 2, 3...$), we have $T_0 = 1$, which is so called transmission resonance. At resonances, and the lateral shift is maximal,

$$s_{max} = s|_{k_{x0}'a=m\pi} = \frac{s_g}{2}\left(\frac{m_2^* k_{x0}}{m_1^* k_{x0}'} + \frac{m_1^* k_{x0}'}{m_2^* k_{x0}}\right).\tag{13}$$

If the incidence angle θ_0 is close to the critical angle θ_c, k_{x0}' is much less than k_{x0}, so that s_{max} is much larger than s_g. On the other hand, when $k_{x0}'a = (m+1/2)\pi$, T_0 reaches its minima and the electron beam is most reflected back. In this case, the lateral shift is also minimal,

$$s_{min} = s|_{k_{x0}'a=(m+1/2)\pi} = 2s_g\left(\frac{m_2^* k_{x0}}{m_1^* k_{x0}'} + \frac{m_1^* k_{x0}'}{m_2^* k_{x0}}\right)^{-1}.\tag{14}$$

Obviously, the GH shift is modulated by the transmission probability T_0, so that it can be greatly enhanced by transmission resonances resulting from the multiple reflections inside the barrier.

In analogy with the negative GH shift in dielectric slab [20], the GH shift of ballistic electrons is found to be negative as well as positive when the electron beam transmits though semiconductor quantum well, as shown in Fig. 2 (c), acting as quantum slab [43]. The expression for the GH shift in quantum well is the same as that for quantum barrier. The only difference considered here is $V_2 < V_1$ for semiconductor quantum well. When the necessary condition

$$\frac{m_2^*}{m_1^*}\frac{k_{x0}}{k'_{x0}} + \frac{m_1^*}{m_2^*}\frac{k'_{x0}}{k_{x0}} < \left(1 - \frac{k'^2_{x0}}{k^2_{x0}}\right)\left(\frac{m_2^*}{m_1^*}\frac{k_{x0}}{k'_{x0}} - \frac{m_1^*}{m_2^*}\frac{k'_{x0}}{k_{x0}}\right), \tag{15}$$

is fulfilled, the GH shift becomes negative, when the incident angle satisfies

$$\cos\theta_0 < \left[\frac{m_2^*(E - V_2)/m_1^*(E - V_1) - 1}{1 + (m_2^*/m_1^*)^2}\right]^{1/2} \equiv \cos\theta_t. \tag{16}$$

Further analysis shows that when the incident energy is in the region of $V_1 < E < E_c$, the necessary condition (16) is satisfied, so that the lateral shift of ballistic electrons in the quantum slab can be negative as well as positive. In other word, if the incidence angle θ_0 is larger than the threshold angle θ_t the GH shifts in transmission through a semiconductor quantum slab can be negative for some values a, width of semiconductor quantum well, while the GH shifts are always positive in the semiconductor quantum barrier ($V_2 > V_1$).

In addition, when $V_2 < V_1$ is assumed for quantum well, there exists the critical angle, θ_c, at the electron energies above E_c. In the case of $E > E_c$, the total internal reflection occurs. Thus, the lateral shifts are always positive, since the necessary condition (16) is invalid. On the contrary, when $E > E_c$ for quantum barrier $V_2 > V_1$, the GH shifts can be negative under some conditions [43]. All these complicated but interesting behaviors result from the effective masses. Note that if the effective masses are equal, $m_1^* = m_2^*$, the critical angle for quantum well does not exist because the critical energy E_c goes to infinity.

Before we turn to the modulation of GH shifts and its applications, we have to clarify the physical explanation of positive and negative GH shifts of ballistic electrons in quantum barrier and well. Originally, the GH shift was explained by the reshaping of totally reflected plane-wave components undergoing different phase shifts, based on Artmann's stationary phase method [4]. The GH shifts presented here can be further understood from the destructive and constructive interference due to the multiple reflections and transmission inside the barrier or well. The negative GH shift is similar to that of light beam transmitted through a dielectric slab [20], but different from that in negatively refractive media [66, 20]. As illustrated in optical analogy, we have already demonstrated that the negative lateral shift is produced by the reshaping effects due to the multiple reflections [23].

2.3. modulation by external fields

From the point of view of applications, the controllability of GH shifts by external fields will provide more flexibility to design the electronic devices, based on the negative and positive shifts mentioned above. To this end, we first focus on the control of GH shift by external electric field, taking account into imposing applied bias field on the semiconductor quantum well, see Fig. 2 (c). Because the system is translationally invariant along the y direction, the
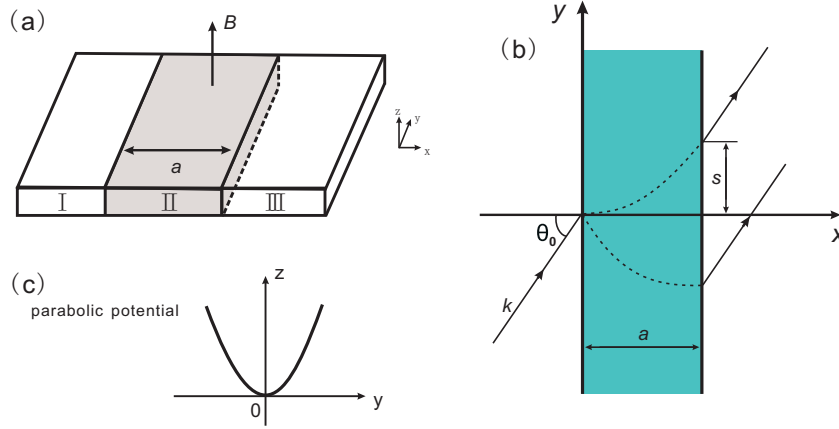
Figure 3. (Color online) (a) Schematic diagram for 2DEG with the parabolic quantum well under a uniform magnetic field B along the vertical z-direction. (b) Negative and positive GH shifts of ballistic electrons are presented in this configuration. (c) Description of the parabolic confinement potential H_{conf}.

wave function in the region of the quantum well under applied electric field can be expressed as $\Psi(x, y) = \psi(x)e^{ik_y y}$, where the longitudinal wave packet is determined by,

$$\frac{\partial^2 \psi(x)}{\partial x^2} + \frac{2m_2^*}{\hbar^2}\left(E_x - V_2 + \frac{eV_a x}{a}\right)\psi(x) = 0, \tag{17}$$

where $E_x = \hbar^2 k_x^2 / 2m_2^*$ is the longitudinal energy and V_a is the applied biased voltage. Generally, the solutions of Schrödinger equation for the Hamiltonian with applied biased voltage V_a are the well-known linearly independent Airy functions $Ai(\eta)$ and $Bi(\eta)$, that is $\psi(x) = MAi(\eta) + NBi(\eta)$, where

$$\eta = \left(-\frac{2m_1^* eV_a}{a\hbar^2}\right)^{1/3}\left[\frac{a}{eV_a}(E_x - V_2) + x\right]. \tag{18}$$

with longitudinal energy $E_x = \hbar^2 k_x^2 / 2m_2^*$. Based on the boundary conditions, the analytical expressions for transmission coefficient and corresponding phase shift are obtained, then the GH shift is finally numerically calculated. In Ref. [43], the numerical results show that the GH shifts with biased voltage can also be negative as well as positive in the same way as those in absence of external applied electric field, and the lateral shifts are tuned from negative to positive when the biased voltage V_a is increased. In addition, we have also illustrated that the parameter χ of semiconductor has great effect on the lateral shifts, when we consider the semiconductor quantum well consisting of $Ga_{1-\chi}Al_\chi As/GaAs/Ga_{1-\chi}Al_\chi As$. Thus, this provides a more feasible scheme to control the GH shifts by using external fields, instead of manipulating the parameters of semiconductor structure, e.g. the width a of quantum well.

Next, we shall discuss that the external magnetic field provide an alternative way to modulate the (negative and positive) GH shifts in quantum well. As depicted as showin Fig. 3, we consider the GH shift for ballistic electrons with total energy E in a parabolic quantum well under a uniform magnetic field, in which the Hamiltonian is given by

$$H = \frac{1}{2m^*}(\mathbf{p} - \mathbf{A})^2 + \frac{1}{2}\mu_B g\sigma B + H_{conf}, \tag{19}$$

with the parabolic confinement energy $H_{conf} = \frac{1}{2}m^*\omega_0^2 y^2$. This system is particularly interesting, because at high magnetic fields, Landau levels form and quantum Hall effect have no any optical analogy [39]. In such a quantum well, the uniform magnetic field bends continuously the trajectory of electron, exhibiting cyclotron motion, which implies that the motion of electron has no direct analogy with the linear propagation of light. But the transmitted electron beam still experiences the GH shift in such quantum systems, and the unique properties of GH shifts depend on not only incident energy and incidence angle, but also the magnetic field and Landau quantum number. After some lengthy but direct calculations, the GH shift in quantum well under a uniform magnetic field is obtained, by using the stationary phase method, as [44]

$$s = \frac{a \tan \theta_0}{2f_0^2}\left(1 - \frac{k_{x0}'^2}{k_{x0}^2}\right)\frac{\sin(2k_{x0}'a)}{2k_{x0}'a},$$

(20)

where the subscript 0 means the value at $k_y = k_{y0}$, that is $\theta = \theta_0$, as before, for the plane wave component under consideration

$$f \exp(i\phi) = \cos(k_x'a) + i\left(\frac{k_x^2 + k_x'^2}{2k_x k_x'}\right)\sin(k_x'a),$$

(21)

the corresponding longitudinal wave vector $k_x = (k^2 - k_y^2)^{1/2}$, and k_x' in the central potential region is

$$k_x' = \sqrt{\frac{2m^*\widetilde{\omega}_c^2[E_n - (n + \frac{1}{2})\hbar\widetilde{\omega}_c - \frac{1}{2}\mu_B g\sigma B]}{\hbar^2\omega_0^2}},$$

(22)

with the parameters: $k = (2m^*E)^{1/2}/\hbar$, effective mass of electron m^*, energy E_n (n is Landau level), cyclotron frequency $\omega_c = Be/m^*$, and $\widetilde{\omega}_c^2 = \omega_0^2 + \omega_c^2$. When the only plane wave is considered, the spatial location inside the potential well is around

$$Y \equiv \hbar k_x'/eB = v(n, k_x')\frac{\omega_0^2 + \omega_c^2}{\omega_c\omega_0^2},$$

(23)

with the velocity

$$v(n, k_x') = \frac{1}{\hbar}\frac{\partial E_n}{\partial k_x'} = \frac{\omega_0^2}{\widetilde{\omega}_c^2}\frac{\hbar k_x'}{m^*}.$$

(24)

The transverse location for each plane wave eigenstate is proportional to the velocity and magnetic field. From the classical viewpoint, the spatial displacement can be plausibly explained by Lorentz force [39]. As a consequence, the transverse shifts for the forward and backward propagating states inside the central region are positive and negative, since Lorentz force is opposite for electrons moving in the opposite direction. However, the lateral displacement predicted by the GH effect will be totally different. On one hand, in the propagating case, when the transmission resonances $k_x'd = m\pi$ or antiresonances $k_x'd = (m + 1/2)\pi$ occur, the GH shift is zero, which means the positions in the y direction are the same for both incident and transmitted electrons. On the other hand, the GH shifts can be negative and positive, depending not only on the incident energy, but also on magnetic field. Whereas, in the evanescent case, the GH shifts become always positive, like in semiconductor

barrier. The dependence of GH shift on the strength of magnetic field and Landau energy level provides more freedom to control the GH shifts. In the propagating case, the GH shifts can be changed from negative to positive by controlling the strength of the magnetic field, and vice versa. However, the GH shifts finally become positive with increasing the strength of the magnetic field, since the propagation of electrons is actually evanescent. Based on these phenomena, the spin beam splitter is proposed in [44], in which the spin-up and spin-down electron beams can be completely separated by negative and positive GH shifts. In addition, we can choose the incident energy within the range of $E_c^+ < E < E_c^-$, where the critical energy for evanescent waves with spin-up and spin-down polarizations are

$$E_c = (n + \frac{1}{2})\hbar\widetilde{\omega}_c + \frac{1}{2}\mu_B g \sigma B, \tag{25}$$

obtained from Eq. (22). This suggests that the spin-down polarized electrons for $E > E_c^-$ can traverse through the structure in the propagating mode with high transmission probability, while the spin-up polarized electrons for $E < E_c^+$ tunnel through it in the evanescent mode with very low transmission probability. These phenomena describes an alternative physical mechanism to design a spin spatial filter with energy gap, $\Delta E = \mu_B g B$. In what follows that we will discuss the applications of GH shifts in spintronics.

2.4. applications in spintronics

Now we shall discuss the spin-dependent GH shift and its application in spintronics. As mentioned before, the proposal for designing spin beam splitter is that the spin-up and spin-down polarized electron beams are separated by different GH shifts in parabolic quantum well under a uniform magnetic field, due to their energy dispersion realtion depending on the spin polarization [44]. In other realistic electronic devices, a significant class of 2DEG nanostructures, magnetic barriers, can be experimentally realized by the deposition of a 2DEG in an inhomogenous field, see the references in [45, 46, 47, 48, 49]. In 2008, we have proposed for the first time the tunable GH shifts and spin beam splitter in the modulation-doped semiconductor heterostructure, depositing two metallic FM stripes on top and bottom of the semiconductor heterostructure [45]. The configuration of such magnetic-electric nanostructure is shown in Fig. 4. The Hamiltonian describing such a system in the (x, y) plane, within the single particle effective mass approximation, is

$$H = \frac{p_x^2}{2m^*} + \frac{[p_y + e\mathbf{A}_y(x)]^2}{2m^*} + U(x) + \frac{eg^*}{2m_0}\frac{\sigma\hbar}{2}B_z(x), \tag{26}$$

where m^* is the electron effective mass and m_0 is the free electron mass, (p_x, p_y) are the components of the electron momentum, g^* is the effective Landé factor, $\sigma = +1/ - 1$ for spin up/down electrons, and $\mathbf{A}_y(x)$ is the y-component of the vector potential given, in Landau gauge, by $\vec{\mathbf{A}} = [0, \mathbf{A}_y(x), 0]$. For GaAs, we can choose $B_z = 0.1$ T, $g^* = 0.44$, and $m^* = 0.067m_0$. Once the Hamiltonian is given, we can follow the similar process to calculate the GH shift in terms of stationary phase method. It was found that the GH shifts of transmitted electron beam are negative and positive, and can be controlled by the magnetic-field strength of ferromagnetic stripes and the applied voltage. Depending on the magnetic
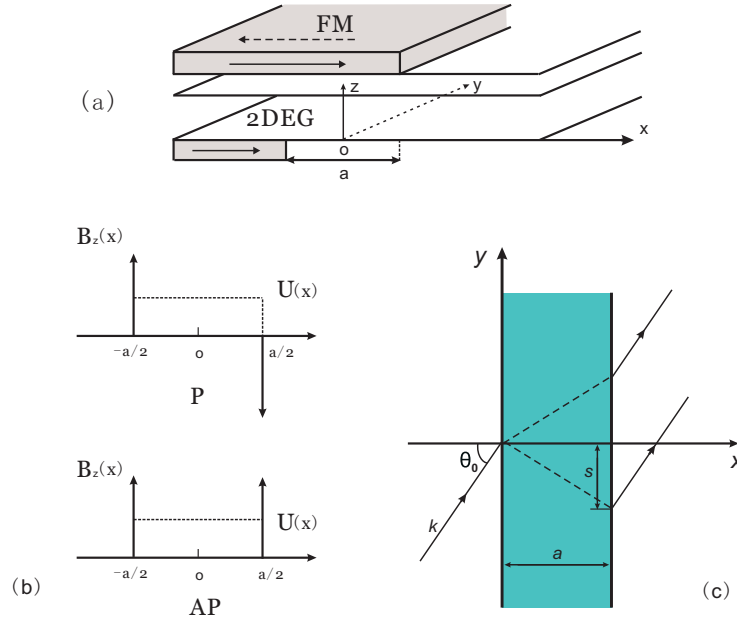
Figure 4. (Color online) (a) Schematic illustration of the magnetic-electric nanostructure with two metallic FM stripes deposited on top and bottom of the semiconductor heterostructure; (b) The magnetic-electric barrier models exploited here corresponds to the P and AP magnetization configurations of two FM stripes, respectively. (c) The positive and negative GH shifts in this nanostructure.

barriers, described by $B_z(x) = B_1\delta(x + a/2) - \chi B_2\delta(x - a/2)$, the behaviors of GH shifts for $\chi = +1$ (P case) and $\chi = -1$ (AP case) are totally different with respect to spin polarization. In the AP configuration, the GH shift depends on the electron spin due to its asymmetry, so that the spin-polarized electron beam can be separated spatially, while in P configuration GH shift does not depend on spin polarization. As a result, the negative and positive GH shifts depend on electron spins when two δ-magnetic barriers point at the same direction, thus a spin beam splitter that separates spin-up and spin-down electron beams by their corresponding GH shifts can be proposed in parallel double δ-magnetic barrier nanostuctures. The proposed spatially separating spin filter and spin beam splitter are different from those designed by the refraction of a spin electron beam at the interface by considering spin-orbit coupling of Rashba and Dresselhaus types [67, 68].

Following the work in [45], Lu's group has also investigated the tunable GH shift and spin beam splitter in the magnetic barrier nanostructure and its variants [46, 47, 48, 49]. For example, the realistic magnetic barriers created by lithographic patterning of ferromagnetic or superconducting film have been further considered [49]. Due to intrinsic symmetry, only nanostructures with symmetric magnetic field possess spin-dependent GH shifts. The control of GH shifts over the incident angle, incident energy, size and position of ferromagnetic stripe is of great benefit to design a new type of spin filter, spin injection, and spin beam splitter in such magnetic-electric nanostuctures.
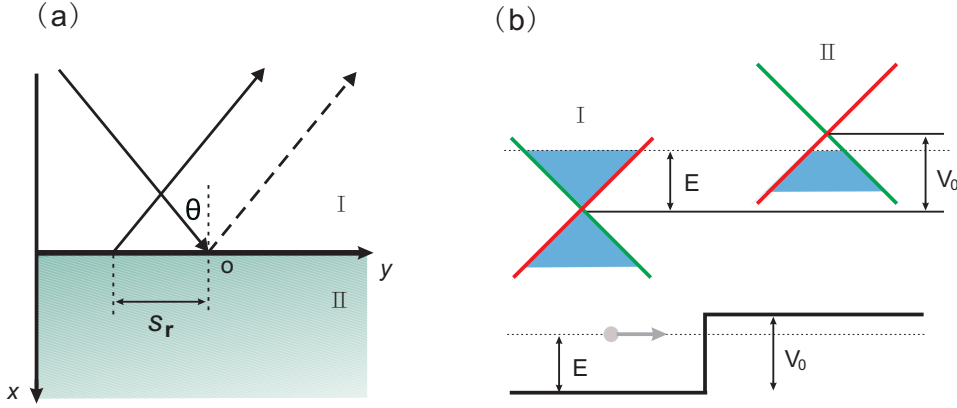
(a)

(b)

Figure 5. (Color online) (a) Schematic diagram of total internal reflection and negative GH shift at a sharp *p-n* junction. (b) Low-energy linear spectrum and potential diagram.

3. Electronic Goos-Hänchen shifts in graphene

3.1. single interface

In this section, we shall turn to the GH shift in graphene, which is different from that in semiconductor. As we know, graphene is a two-dimensional zero-gap semiconductor with linear dispersion relation, $E = \hbar k v_F$, thus the low-energy quasi-particles are formally described by the Dirac-like Hamiltonian [60], $\hat{H}_0 = -i\hbar v_F \sigma \cdot \nabla$, $v_F \approx 10^6 m \cdot s^{-1}$ is the Fermi velocity, k is the Fermi wave vector, and $\sigma = (\sigma_x, \sigma_y)$ are the Pauli matrices. The linear energy dispersion and two spinor component of the wave function differentiate the electron wave propagation in graphene from that in semiconductor, which leads to many interesting optic-like phenomena, such as negative refraction [62], collimation [69], Fabry-Perot interference [70], Bragg reflection [71] and waveguide [72]. To consider the GH shift in graphene, the incident electron beam is assumed to be

$$\Psi_{in} = \int_{-\infty}^{\infty} dk_y A(k_y - k_{y0}) e^{i(k_x x + k_y y)} \begin{pmatrix} e^{-i\theta/2} \\ e^{i\theta/2} \end{pmatrix}, \tag{27}$$

and the reflected one is thus expressed as

$$\Psi_r = \int_{-\infty}^{\infty} dk_y r(k_y) A(k_y - k_{y0}) e^{i(-k_x x + k_y y)} \begin{pmatrix} -ie^{i\theta/2} \\ ie^{-i\theta/2} \end{pmatrix}, \tag{28}$$

where $A(k_y - k_{y0})$ is the angular spectral distribution around the central wave vector k_{y0} and the reflection amplitude is $r(k_y) = |r| \exp[i\phi_r(k_y)]$. The two upper and lower components $\Psi_{in,\pm}$ at the interface $x = 0$ centered at two different mean y coordinates, $\bar{y}_\pm^{in} = \pm\frac{1}{2}\theta'(k_{y0})$. The two components $\Psi_{r,\pm}$ at the interface $x = 0$ centered at $\bar{y}_\pm^r = -\phi_r'(k_{y0}) \mp \frac{1}{2}\theta'(k_{y0})$. So the upper spinor component displaced along the interface by an amount $\sigma_+ = \bar{y}_+^r - \bar{y}_+^{in} = -\phi_r'(k_{y0}) - \theta'(k_{y0})$, while the displacement of lower spinor component is given by $\sigma_- = \bar{y}_-^r - \bar{y}_-^{in} = -\phi_r'(k_{y0}) + \theta'(k_{y0})$. Different from that in semiconductor, the GH shift in graphene is defined as

$$s_r = \frac{1}{2}(\sigma_+ + \sigma_-) = -\frac{\partial \phi_r}{\partial k_y}|_{k_y = k_{y0}}, \tag{29}$$

which means the average displacement of upper and lower spinor components. Noting that different spin component for incident wave will lead to different definition of GH shift in graphene. In order to clarify the difference from the GH shift in semiconductor, we would like to repeat the calculations of GH shift in the literatures [50, 51]. As shown in Fig. 5, we consider the incident electron wave with incidence angle θ. Based on the Dirac-like equation described above, we can write down the wave functions in the two different regions of I and II. By defining $k = |E|/\hbar v_F$ and $k' = |E - V_0|/\hbar v_F$, we have

$$\psi_I = \frac{1}{\sqrt{2}} \begin{pmatrix} e^{-i\theta/2} \\ se^{i\theta/2} \end{pmatrix} e^{ik_x x + ik_y y} + \frac{r}{\sqrt{2}} \begin{pmatrix} -ie^{i\theta/2} \\ sie^{-i\theta/2} \end{pmatrix} e^{-ik_x x + ik_y y}, \tag{30}$$

with $k_x = k \cos\theta$, $k_y = k \sin\theta$, and $s = \text{sgn}(E)$, where r is the reflection amplitude. In region II, the transmitted wave is given by

$$\psi_{II} = \frac{t}{\sqrt{2}} \begin{pmatrix} e^{-i\varphi/2} \\ s'e^{i\varphi/2} \end{pmatrix} e^{ik'_x x + ik_y y}, \tag{31}$$

with $k'_x = k' \cos\varphi$ and $s' = \text{sgn}(E - V_0)$. By using boundary conditions at $x = 0$, we can calculate the coefficients r and t, where r is given by

$$r = \frac{i(e^{i\theta} - ss'e^{i\varphi})}{1 + ss'e^{i\theta}e^{i\varphi_r}}. \tag{32}$$

When the incidence angle θ is larger than critical angle $\theta_c = \arcsin|V_0/E - 1|$, the total reflection occurs. In this case, $k'_x = i\kappa = i(k_y^2 - k'^2)^{1/2}$, the reflection coefficient becomes

$$r = |r| \exp[i\phi_r(k_y)] = \frac{ie^{i\theta}ss'k' + (\kappa + k_y)}{ss'k' + ie^{i\theta}(\kappa + k_y)}. \tag{33}$$

According to the above definition (29), the GH shift at the single interface, as shown in Fig. 5, is obtained as [50]

$$s_r = \frac{1}{\kappa_0} \frac{k_{y0}^2 + ss'k^2(|V_0/E - 1|)}{k_{x0}k_{y0}}. \tag{34}$$

Noting that 0 in the subscript means the value at $k_y = k_{y0}$ and the GH shift in total reflection is again the order of electron wavelength, $1/\kappa_0$. In general, when graphene *n-n* interface (when $E > V_0$) is considered, $ss' = 1$, thus the GH shift is always positive, like the GH shift at the single semiconductor interface. Interestingly, the negative GH shift appears at a graphene *p-n* interface (when $E < V_0$), due to $ss' = -1$, for the incidence angles satisfying

$$\theta_c < \theta_0 < \theta^* = \arcsin\sqrt{\sin\theta_c}. \tag{35}$$

On the contrary, when $\theta_0 > \theta^*$, the GH shift becomes positive, regardless of the relative magnitude of E and V_0.

To understand the positive and negative GH shifts in graphene, we may define the effective refractive index as $n_e = E/(E - V_0)$. In the case of $E < V_0$, the Klein tunneling is analogous to the phenomenon of negative refraction in metamaterial with $n_e < 0$. On the contrary, the classical motion for $E > V_0$ corresponds to the positive refractive index ($n_e > 0$) in the normal dielectric. Since the link between Klein tunneling and negative refraction, many intriguing phenomena in metamaterial, for example, negative refraction, Veselago lens and

focusing [62], have been transferred to the electron transports in graphene. In addition, the optical analogy of graphene has been also proposed in photonic crystals [73, 74, 75] and negative-zero-positive index metamaterial (NZPIM) [76, 77]. For more information, we refer the readers to the recent review in [78].

3.2. single, double and multiple barriers

Recent publications have shown that the GH shifts in graphene can be greatly enhanced by transmission resonances in various graphene-based nanostructures including single [52], double [53] and multiple barriers [54].

In graphene-based barrier, the expression of GH shift are similar to that in semiconductor barrier, so we will not repeat them. But since the unique properties of electron transport in graphene, the GH shifts are simply discussed in two difference cases: Klein tunneling and classical motion [79]. In classical motion, the critical angle becomes

$$\theta_c = \arcsin\left(1 - \frac{V_0}{E}\right), \tag{36}$$

when $E > V_0$ is satisfied. Thus, the electron wave propagations can be propagating and evanescent cases, which depend on the incidence angle below or above the critical angle for total reflection. In both cases, the GH shifts are always positive as those in the 2D semiconductor barrier [42]. In Klein tunneling case, there is a critical angle for total reflection, defined as

$$\theta_c = \arcsin\left(\frac{V_0}{E} - 1\right), \tag{37}$$

when the condition $E < V_0 < 2E$ is satisfied. When the incidence angle θ_0 is less than the critical angles θ_c, that is, $\theta_0 < \theta_c$, the GH shifts can be positive as well as negative. Particularly, the lateral shifts can be positive for a thin barrier, while at some resonance or anti-resonance points they become negative. And the negative lateral shifts can be enhanced by the transmission resonances. When $\theta_0 > \theta_c$, the GH shift in the evanescent case is about the order of electron wavelength, and becomes independent of barrier's thickness. More interestingly, the saturated GH shift is negative when the incidence angle satisfies $\theta_c < \theta_0 < \theta^*$, while it becomes positive when $\theta_0 > \theta^*$. This result is related to pseudospin degree, as mentioned in [50]. As a consequence, the sign change of the GH shifts appears at different incidence angles, which also provides the freedom to control the GH shift. As a matter of fact, the positive and negative GH shifts discussed here remind us those of light beam transmitted through a slab of negative-index metamaterial [20]. In the slab of negative-index metamaterial, the negative index contributes to the negative lateral shift, while the positive lateral shift does result from the reshaping effect due to the multiple reflections. This provides the physical explanation of positive and negative GH shifts in the graphene barrier, which is totally different from those in semiconductor quantum slab [43]. In semiconductor quantum slab, the negative lateral shift has nothing to do with Klein tunneling (negative refraction in the language of optics), and does originate from the beam reshaping resulting from multiple reflections inside the slab [20]. Our recent work is devoted to the optical simulation of transmission gap and Klein

tunneling in graphene barrier [22], by using the negative-zero-positive index metamaterial (NZPIM) [76, 77], in which the similar negative and positive GH shifts, relevant to Klein tunneling and classical motion, are also found.

Most recently, the GH shifts in graphene-based barrier are directly generalized to graphene double barrier and multiple barrier (superlattice) structures. Different from the GH shifts in graphene barrier, the GH shifts in double barrier structure can be greatly enhanced [53] inside the transmission gap in a single barrier [52, 79]. This giant GH shift is attributed to the quasibound states formed in double barriers. Moreover, they have made the conclusion that the smoothness of the potential barrier will not restrict the application of the giant GH shifts, by studying a realistic potential which varies smoothly on the scale of the graphene lattice constant. (We should point out that the similar analysis of electronic GH shifts is also interesting for the smooth interfaces in semiconductor.) In subsequent work, we have also investigated the giant negative and positive lateral shifts for the transmitted electron beam through monolayer graphene superlattices [54]. The GH shifts, depending on the location of new Dirac point, can be negative as well as positive. Especially when the condition $q_A d_A = -q_B d_B = m\pi$ ($m = 1, 2, 3...$) is satisfied, the lateral shifts can be controlled from negative (positive) to positive (negative) when the incident energy is above (below) the Dirac point, by increasing the incidence angle. In addition, the lateral shifts can be greatly enhanced by the effect of defect mode inside the zero-$\bar{k}$ bandgap. Actually, the optical analogy of giant GH shifts in graphene superlattice can be realized near the band-crossing structure of one-dimensional photonic crystals containing left-handed metamaterials [80]. In a word, the tunable and giant GH shifts will have potential applications in the graphene-based electron wave devices, such as electronic wave filter and beam splitter.

3.3. strain effect

As far as we know, the GH shifts in graphene can be tuned by external electric and magnetic fields. For example, Sharma and Ghosh [55] have studied the electronic GH shifts in terms of the analogy between light propagation and electron transport in graphene. The GH shifts are shown to be controlled by adjusting electric and magnetic barriers. In recent years, more attention has been paid on mechanical strain, which induces a pesudo-vector potential, and can be used to manipulate electron transport without using external fields. Motivated by these progresses, Chang *et. al.* [56] have demonstrated that the electrons in opposite valleys (K and K') show different Brewster-like angles and GH shifts, by engineering of local strains. In the strained graphene, the low-energy electrons can be well described by the effective Hamiltonian $H = v_F \sigma^i \cdot (p + \xi A^i / v_F) + V^i$, where the superscript i indicates the different regions, V^i is the electrostatic potential in the region i, $\xi = \mp 1$ labels K and K' valleys, and the Landau gauge $\mathbf{A} = (0, A_y, 0)$ is used here. Here we focus on the analogy between the strained graphene and metamaterial. For simplicity, $V^i = 0$ can be set, since the valley-dependent Brewster angle is the gauge vector ξA. Let us start by considering electron with $k = E/\hbar v_F$ reflection from a region of uniform uniaxial strain. In the strained region, we have

$k_{x,\xi}^2 + (k_y + \xi A_y)^2 = k^2$, so that the critical angle for total reflection is

$$\theta_{c,\xi} = \arcsin\left(\frac{k_y + \xi A_y}{k}\right), \tag{38}$$

and the effective refractive index in optics can be defined as $n_{e,\xi} = (k_y + \xi A_y)/k_y$. Note that when $k_y(k_y + \xi A_y) < 0$, the refractive index of the strained graphene is negative just like for a metameterial with negative refractive index. As pointed out in Ref. [56], the refractive index can be tuned mechanically in a large range, which is not so for the metamaterial in optics. Besides, the perfect transmission through a region of uniform uniaxial strain with width D has different windows in the K or K' valley, since the above critical angle has a different dependence on the vector potential for two valleys denoted by $\xi = \pm 1$. For some incidence angles, we can achieve totally transmitted electron beams for one valley and totally reflected electron beams for the other valley simultaneously. These characteristic angles are further analogous to the so-called Brewster angle in optics. Going back to the case of single interface, we apply stationary phase method, and calculate the GH shift for a uniform uniaxial strain in graphene [56]

$$s_r = \frac{2k_{y0} + \xi A_y}{k_{x0}\kappa_{0\xi}}, \tag{39}$$

from the reflection coefficient

$$r = \frac{k_x + i(k_y - k_y' - \kappa)}{k_x - i(k_y - k_y' - \kappa)} = e^{i2\phi_r(k_y)}, \tag{40}$$

and phase shift

$$\phi_r(k_y) = \arctan\left(\frac{k_y - k_y' - \kappa}{k_x}\right), \tag{41}$$

with $k_y' = k_y + \xi A_y$ and $\kappa = (k_y'^2 - k^2)^{1/2}$ for the total reflection when incidence angle above the critical angle. Again the subscript 0 means the value at $\theta = \theta_0$, where θ_0 is the incidence angle of electron beam, and θ is the incidence angle of plane wave under consideration. Clearly, the GH shifts can be positive or negative, and the strain effect will provide the totally different scheme to control the GH shift in graphene, which is different from the control of GH shifts by external electric [50] and/or inhomogeneous magnetic field [44, 45]. This valley-dependent GH shift will further give rise to the application in valleytronics [57, 58]. Exhibiting a close analogy with optical GH shift in dielectric slab [20], the GH shift of the transmitted electron beam for a normal/strained/nomal graphene junction can be further remarkably enhanced by the valley-dependent transmission resonances, which has been already utilized to design a valley beam splitter in [57].

Finally, we shall emphasize that the strain effect really provides a useful way to tune GH shifts in graphene, as compared to the controllability in semiconductor. The two valleys in graphene are related by time reversal symmetry and act in much the same way as electron spin in spintronics. So valley-dependent GH shift and its modulation in graphene might be useful in graphene-based devices, referred to as valleytronics. Thus this research line is promising and still worthwhile explored. One can further consider the valley-dependent GH shifts in (gapped) graphene with spin-orbit coupling and bilayer graphene, as the extension in [52, 81].

4. Summary and outlook

We have reviewed the electronic GH shifts in semiconductor and graphene-based nanostructures, including single, double barriers and superlattices. The common feature is that the GH shift can be enhanced by transmission resonances, and the (negative or positive) lateral shifts can be controlled by various approaches. From the point of view of application, the controllability of GH shifts can be realized by using external electric/magnetic fields in semiconductor and even by adjusting strain in graphene. The spin (or valley)-dependent GH shifts also open the new possibility to design the electronic devices, such as spin (or valley) beam splitters and filters.

Usually the analogies between phenomena occurring in two different physical systems open a route to find new effects or tow translate techniques or devices, and quite often help to understand both systems better. In this emerging field, we have gained an increased understanding and intriguing phenomena, and new physical effects of electronic GH shifts. However, there still exist several open questions. For the application, the measurement of electronic GH shifts for electron beams in semiconductor or graphene remains challenging with several possible reasons, for example, preparation of required (well-collimated) electron beams, electron scattering, the smoothness of potential, and the smallness of GH shifts. These imply the electronic systems are different and more complicated, which sets the limits of the optical analogy in solid state. For example, in the recent experiment on electron waveguide in graphene [72], the GH shift is about 1 nm ($\simeq 2\pi/k$) under typical doping conditions. With the estimated disorder to be of the same order of few nanometer, hence it is impossible to observe the signature of GH effect, i.e. a quantized conductance of $8e^2/h$ at guide thickness of 1.5 nm [50]. Theoretically, the electronic GH shift may have the close connection with the electron transport in semiconductor and graphene, since there is a hint that the lateral and angular GH shifts are analogous to the skew scattering and side jump [84], but without pursuing (see Fig. 8.4 in reference [84]). Therefore, the spin-dependent GH shifts are considered to be relevant to anomalous Hall effect [82, 83]. But so far the spin-dependent GH shifts presented in this review have nothing to do with the spin-orbit coupling. So the spin-dependent GH shift and relevant electronic transport in presence of spin-orbit coupling might be extremely interesting and significant for further work, and will definitely help to understand the beam shifts and spin-orbit coupling in optics.

Last but not least, recent theoretical prediction [85] and experimental realization [86, 87] on (GH or IF) beam shifts, electron vortex beams carrying orbital angular momentum pave new avenues to investigate angular momentum, spin-orbit interaction [88], and relativistic analogy of spin Hall effect [89], which are beyond the scope of this review but worth mentioning.

References

[1] F. Goos and H. Hänchen, Ann. Phys. (Leipzig) **1**, (1947) 333; **5**, (1949) 251.

[2] H. K. V. Lotsch, Optik (Stuttgart) **32**, (1970) 116; **32**, (1970) 189; **32**, (1971) 299; **32**, (1971) 553.

[3] Newton, Isaac. Opticks: A Treatise of the Reflexions, Refractions, Inflexions and Colours of Light. London: Royal Society, 1704.

[4] K. V. Artmann, Ann. Phys. (Leipzig) **2**, (1948) 87.

[5] R.-H. Renard, J. Opt. Soc. Am. **54**, (1964) 1190.

[6] T. Sakata, H. Togo, and F. Shimokawa, Appl. Phys. Lett. **76**, (2004) 2814.

[7] X. B. Yin and L. Hesselink, Appl. Phys. Lett. **89**, (2006) 261108.

[8] T.-Y. Yu, H.-G. Li, Z.-Q, Cao, Y. Wang, and Q.-S. Shen, Y. He, Opt. Lett. **33**, (2008) 1001.

[9] A. M. Steinberg and R. Y. Chiao, Phys. Rev. A **49**, (1994) 3283.

[10] A. A. Stahlhofen, Phys. Rev. A **62**, (2000) 012112.

[11] Ph. Balcou and L. Dutriaux. Phys. Rev. Lett. **78**, (1997) 851.

[12] A. K. Ghatak, M. R. Shenoy, I. C. Goyal, and K. Thyagarajan, Opt. Commun. **56**, (1986) 313.

[13] A. Haibel, G. Nimtz, and A. A. Stahlhofen, Phys. Rev. E **63**, (2001) 047601.

[14] X. Chen, C.-F. Li, R.-R. Wei, and Y. Zhang, Phys. Rev. A **80**, (2009) 015803.

[15] X. Chen, X.-J. Lu, P.-L. Zhao, and Q.-B. Zhu, Opt. Lett. **37**, (2012) 1526.

[16] X. Yin, L. Hesselink, Z. Liu, N. Fang, and X. Zhang, Appl. Phys. Lett. **85**, (2004) 372.

[17] F. Pillon, H. Gilles, S. Girard, M. Laroche, R. Kaiser, and A. Gazibegovic, J. Opt. Soc. Am. B **22**, (2005) 1290.

[18] C. W. Hsue and T. Tamir, J. Opt. Soc. Am. A **2**, (1985) 978.

[19] R. P. Riesz and R. Simon, J. Opt. Soc. Am. A **2**, (1985) 1809.

[20] C.-F. Li, Phys. Rev. Lett. **91**, (2003) 133903; X. Chen and C.-F. Li, Phys. Rev. E **69**, (2004) 066617.

[21] D. Müller, D. Tharanga, A. A. Stahlhofen, and G. Nimtz, Europhys. Lett. **73**, (2006) 526.

[22] X. Chen, L.-G. Wang, and C.-F. Li, Phys. Rev. A **80**, (2009) 043839.

[23] X. Chen and C.-F. Li, J. Opt. A: Pure Appl. Opt. **11**, (2009) 085004.

[24] R. Briers, O. Leroy, and G. Shkerdinb, J. Acoust. Soc. Am. **108**, (2000) 1624.

[25] V. K. Ignatovich, Phys. Lett. A **322**, (2004) 36.

[26] Victor-O. deHaan, J. Plomp, Theo M. Rekveldt, W. H. Kraan, Ad A. van Well, R. M. Dalgliesh, and S. Langridge, Phys. Rev. Lett. **104**, (2010) 010401.

[27] J.-H. Huang, Z.-L. Duan, H.-Y. Ling, and W.-P. Zhang, Phys. Rev. A **77**, (2008) 063608.

[28] F. I. Fedorov, Dokl. Akad. Nauk SSSR **105**,(1955) 465.

[29] C. Imbert, Phys. Rev. D **5**, (1972) 787.

[30] O. Costa de Beayregard and C. Imbert, Phys. Rev. Lett. **28**, (1972) 1211.

[31] C.-F. Li, Phys. Rev. A **76**, (2007) 013811.

[32] O. Hosten and P. Kwiat, Science **319**, (2008) 787.

[33] A. Aiello, N. Lindlein, C. Marquardt, and G. Leuchs, Phys. Rev. Lett. **103**, (2009) 100401.

[34] K. Y. Bliokh and Andrea Aiello, arXiv:1210.8236, J. Opt. A (accepted).

[35] J. L. Carter and H. Hora, J. Opt. Soc. Am. **61**, (1971) 1640.

[36] S. C. Miller, Jr., and N. Ashby, Phys. Rev. Lett. **29**, (1972) 740.

[37] D. M. Fradkin and R. J. Kashuba, Phys. Rev. D **9**, (1974) 2775; **10**, (1974) 1137.

[38] T. K. Gaylord, E. N. Glytsis, G. N. Henderson, K. P. Martin, D. B. Walker, D. W. Wilson, and K. F. Brennan, Proc. IEEE **79**, (1991) 1159, and references therein.

[39] S. Datta, *Electronic Transport in Mesoscopic Systems*, Cambridge University Press, New York, (1996) 276.

[40] D. Dragoman and M. Dragoman, Progress in Quantum Electronics **23**, (1999) 131.

[41] D. W. Wilson, E. N. Glytsis, and T. K. Gaylord, IEEE J. Quantum Electron. **29**, (1993) 1364.

[42] X. Chen, C.-F. Li, and Y. Ban, Phys. Lett. A **354**, (2006) 161.

[43] X. Chen, Y. Ban, and C.-F. Li, J. Appl. Phys. **105**, (2009) 093710.

[44] X. Chen, X.-J. Lu, Y. Wang, and C.-F. Li, Phys. Rev. B **83**, (2011) 195409.

[45] X. Chen, C.-F. Li, and Y. Ban, Phys. Rev. B **77**, (2008) 073307.

[46] L. Yuan, M.-W. Lu, Y.-H. Zhao, and L.-H. Shen, Phys. Lett. A **375**, (2011) 4198.

[47] L. Yuan, L.-L. Xiang, Y.-H. Kong, M.-W. Lu, Z.-J. Lan, A.-H. Zeng, and Z.-Y. Wang, Eur. Phys. J. B **85**, (2012) 1434.

[48] Y.-H. Kong, M.-W. Lu, S.-Y. Chen, and G.-L. Zhang, J. Magn. Magn. Mater. **324**, (2012) 2519.

[49] M.-W. Lu, G.-L. Zhang, and S.-Y. Chen, J. Appl. Phys. **112**, (2012) 014309.

[50] C. W. J. Beenakker, R. A. Sepkhanov, A. R. Akhmerov, and J. Tworzydło, Phys. Rev. Lett. **102**, (2009) 146804.

[51] L. Zhao and S. F. Yelin, Phys. Rev. B **81**, (2010) 115441.

[52] X. Chen, J.-W. Tao, and Y. Ban, Eur. Phys. J. B **79**, (2011) 203.

[53] Y. Song, H.-C. Wu and Y. Guo, Appl. Phys. Lett. **100**, (2012) 253116.

[54] X. Chen, P.-L. Zhao, X.-J. Lu, and L.-G. Wang, arXiv.1111.1753.

[55] M. Sharma and S. Ghosh, J. Phys.: Condens. Matter **23**, (2011) 055501.

[56] Z. Wu, F. Zhai, F. M. Peeters, H. Q. Xu, and K. Chang, Phys. Rev. Lett. **106**, (2011) 176802.

[57] F. Zhai, Y.-L. Ma, and K. Chang, New J. Phys. **13**, (2011) 083029.

[58] Z.-Z. Cao, Y.-F. Cheng, and G.-Q. Li, Physica B **407**, (2012) 4254.

[59] K. S. Novoselov, A. K. Geim, S. V. Morozov, D. Jiang, Y. Zhang, S. V. Dubonos, I. V. Grigorieva, and A. A. Firsov, Science **306**, (2004) 666.

[60] See review: A. H. Castro Neto, F. Guinea, N. M. R. Peres, K. S. Novoselov, and A. K. Geim, Rev. Mod. Phys. **81**, (2009) 109.

[61] H. Raza, *Graphene Nanoelectronics*, Springer, Berlin Heidelberg 2012, Charpt. 15.

[62] V. V. Cheianov, V. Fal'ko, and B. L. Altshuler, Science **315**, (2007) 1252.

[63] D. Bohm, *Quantum Theory*, Prentice-Hall, New York, 1951, p. 259.

[64] D. Dragoman and M. Dragoman, *Quantum-classical analogies*, Springer, 2004.

[65] D. Dragoman and M. Dragoman, J. Appl. Phys. **101**, (2007) 104316.

[66] P. R. Berman, Phys. Rev. E **66**, (2002) 067603; **71**, (2005) 039903(E).

[67] M. Khodas, A. Shekhter, and A. M. Finkel'stein, Phys. Rev. Lett. **92**, (2004) 086602.

[68] X.-D. Zhang, Appl. Phys. Lett. **88**, (2006) 052114.

[69] C. H. Park, Y. W. Son, L. Yang, M. L. Cohen, and S. G. Louie, Nano Lett. **8**, (2008) 2920.

[70] A. V. Shytov, M. S. Rudner, and L. S. Levitov, Phys. Rev. Lett. **101**, (2008) 156804.

[71] S. Ghosh and M. Sharma, J. Phys.: Condens. Matter, **21**, (2009) 292204.

[72] J. R. Williams, T. Low, M. S. Lundstrom, and C. M. Marcus, Nature Nanotech. **6**, (2011) 222.

[73] F. D. M. Haldane and S. Raghu, Phys. Rev. Lett. **100**, (2008) 013904.

[74] O. Peleg, G. Bartal, B. Freedman, O. Manela, M. Segev, and D. N. Christodoulides, Phys. Rev. Lett. **98**, (2007) 103901.

[75] R. A. Sepkhanov, Y. B. Bazaliy, and C. W. J. Beenakker, Phys. Rev. A **75**, (2007) 063813.

[76] L.-G. Wang, Z.-G. Wang, J.-X. Zhang, and S.-Y. Zhu, Opt. Lett. **34**, (2009) 1510.

[77] L.-G. Wang, Z.-G. Wang, and S.-Y. Zhu, Europhys. Lett. **86**, (2009) 47008.

[78] X. Chen and L.-G. Wang, (2011) Propagation of Electron Waves in Monolayer Graphene and Optical Simulations with Negative-Zero-Positive Index Metamaterials, *Physics and Applications of Graphene-Theory*, S. Mikhailov (Ed.), ISBN: 978-953-307-152-7, InTech.

[79] X. Chen and J.-W. Tao, Appl. Phys. Lett. **94**, (2009) 262102.

[80] L.-G. Wang and S.-Y. Zhu, Appl. Phys. B **98**, (2010) 459.

[81] M. Cheng, Eur. Phys. J. B **85**, (2012) 89.

[82] N. A. Sinitsyn, Q. Niu, J. Sinova, and K. Nomura, Phys. Rev. B **72**, (2005) 045346.

[83] K. Yu. Bliokh and V. D. Freilikher, Phys. Rev. B **74**, (2006) 174302.

[84] M. I. Dyakonov, Spin Physics in Semiconductors, Series: Springer Series in Solid-State Sciences, Vol. 157, 2008.

[85] K. Y. Bliokh, Y. P. Bliokh, S. Savelév, and F. Nori, Phys. Rev. Lett. **99**, (2007) 190404.

[86] M. Uchida and A. Tonomura, Nature **464**, (2010) 737.

[87] J. Verbeeck, H. Tian, and P. Schattschneider, Nature **467**, (2010) 301.

[88] K. Y. Bliokh, M. R. Dennis, and F. Nori, Phys. Rev. Lett. **107**, (2011) 174802.

[89] K. Y. Bliokh and F. Nori, Phys. Rev. Lett. **108**, (2012) 120403.